arXiv:cond-mat/0507494v1 [cond-mat.str-el] 21 Jul 2005

One-band Hubbard model with hopping asymmetry and the effect theory at finite U: Phase diagram and metal-insulator transition

Yuchuan Wen[1] and Yue Yu[1]

[1] *Institute of Theoretical Physics, Chinese Academy of Sciences, P.O. Box 2735, Beijing 100080, China*

(Dated: February 2, 2008)

We study the one-band Hubbard model at half filling with hopping asymmetry and its effective model at finite but large U up to the second order of t/U. Two variational wave functions, the resonating valence bond (RVB) wave function and anti-ferromagnetic-RVB(AF-RVB) coexisted wave function, are studied by variational Monte Carlo method on L×L square lattices up to L=12. Based on these two wave functions, the phase diagrams for both models are presented. For the Hubbard model, we find that there is a metal-insulator transition when the hopping parameter t_{mix} which changes the local double occupant vanishes while only a metal-insulator crossover is explored for any finite t_{mix}. For the effective model in which the perturbation expansion is up to the second order of t_{mix}/U, a clear metal-insulator transition can be identified for both variational wave functions and the phase diagram can be drawn accordingly. In both models, we find that the systems are dominated by AF-RVB wave function when U is large while RVB wave function is favored when U is small.

PACS numbers: PACS numbers: 74.20.-z,74.20.Mn,71.10.Fd

I. INTRODUCTION

The one-band Hubbard model is a generic model for interacting electrons in the narrow-band and strongly correlated systems[1]. Especially, since the high temperature superconductivity was discovered in the cuprates, the Hubbard model on two-dimensional lattices as well as its strong coupling limit model[2], the t-J model, have been extensively studied in order to understand the various anomalous properties of the cuprate superconductor. The up-date investigations, however, can not supply a definitive evidence to show the stable d-wave superconducting ground state in these strongly correlated models[3].

It was known that since the Hubbard model for two-dimensions is not exactly solvable, using the Hubbard model to study the exchange correlation of the system is difficult. On the other hand, the t-J model is weaker in studying the long range charge correlation because the on-site Coulomb repulsion becomes trivial due to the non-doubly occupied projection. A better phenomenological model to include stronger correlations is the t-J-U model[4]. The existence of both J- and U- terms is very important in a possible new mechanism of superconductivity, gossamer superconductivity, proposed by Laughlin recently[3,5,6]. Both J and U appearing in the model has been argued to be the result of the correlations like charge transfer processes in the three band Hubbard model[7]. Dealing with the three-band Hubbard model, however, is very complicated and thus, the precise analytical deduction from the three band to single band Hubbard models lacks. Moreover, an exact reduction from the three band model to the single band with both J and U terms are more difficult.

In this paper, we would like to deal with the one-band Hubbard model with a hopping asymmetry at finite U. In this case, since the on-site Coulomb repulsion is not infinite, there may be a fraction of the lattice sites doubly occupied by electrons. Thus, the U-term is non-trivial but can be exactly treated. The difficulty is to deal with the kinetic term. We will present a variational Monte Carlo calculation for the Hubbard model in a two-dimensional square lattice. We examine two types of variational wave functions, the resonating valence bond (RVB) wave function and anti-ferromagnetic-RVB (AF-RVB) coexisted wave function. There are many variational wave functions, including AF, RVB and AF-RVB, due to different kind of approximation. The early studies shows that the results of AF and RVB were contradictory but the AF-RVB had lower energy[14,16]. So it is quite reasonable to consider the AF-RVB wave function. However, the mean field studies prefer RVB[5,15]. So we included RVB in our work that it might get a comparison with the mean field studies. It is found that the RVB state has a lower variational energy for smaller U and t_{mix} which is the hopping amplitude changing the local double occupation while the AF-RVB state is favorite for larger U and t_{mix}. For both wave functions, we check their phase structures. Both wave functions have a crossover from metal to insulator states as U/t_{mix} tends to infinity. On the other hand, there is an ambiguity to find an optimal variational paring parameter Δ describing the RVB feature of the states. In a wide range from $\Delta = 0$ to 1, the variational energies are almost degenerate for the lattice size in our calculation. This leads to a difficulty to identify if the metal state is either Fermi liquid or d-wave superconducting.

To understand the physics in the crossover regime more clearly, we study an effective model which includes the contribution up to the second order of t_{mix}/U. Moreover, the experience in the t-J model taught us, if there is a spin exchange term in the Hamiltonian, the pairing variational parameter is much easier to be optimized[9]. For a large U, the spin exchange may be explicitly shown

by considering the virtual hopping of electron between two single occupied sites. A hopping term changing the double-occupancy may be taken as a perturbation as that in deducing the t-J model from the single band Hubbard model. In the perturbative deduction from the Hubbard model to the t-J model, we see that the J-term is actually from the second order perturbation in t_{mix}/U by taking the off-diagonal term for the double-occupied number in the kinetic term as the perturbation Hamiltonian. Namely, if the t-term is decomposed into $T_{\rm diag} + T_{\rm off-diag}$, the perturbation process transfers $T_{\rm off-diag}$ to J-term, a virtual hopping process, and only $T_{\rm diag}$ serves as the real hopping[10]. It can also clearly be seen from the canonical transformation deduction of the t-J model[11]. In the present case, we can still have a J term as in the t-J model while the U term is kept due to a non-zero double-occupancy. In the t-J model, due to the no-double occupancy constraint, the kinetic term is a hopping between a single-occupied site to an empty site. For the present model, besides this hopping term, a hopping between double- and single-occupied sites and a pair hopping between the double-occupied and empty sites would be included. Thus, we can derive an effective theory at large but finite U, which captures both the charge and exchange correlations of the system. We can have kinetic, J- and U- terms. However, it should not confuse with the t-J-U model mentioned above. In t-J-U model, the J is set as a free parameter that means J is independent of t and U[7]. But in our case, J comes from the expansion of t_{mix}/U. In this effective theory, there is no a hopping term which changes the local double occupation. It is an extension of the t-J model with doubly-occupied sites.

To work out our model, we use the canonical transformation. We find that, to the second order of t_{mix}/U, the effective Hamiltonian can be written as the sum over the Hamiltonians acting on a subspace of the Hilbert space with a fixed double occupied number D. This fixed D Hamiltonian including three hopping terms which serve the electron hopping from single to empty sites (t_h term), double to single sites (t_d term), and the paring hopping (t_p term); the U term and J-term as well as various nearest neighbor interactions.

We also study the RVB and AF-RVB variational wave functions for this effective model by the variational Monte Carlo method. The RVB state is in smaller J and U regime while AF-RVB state is favored in larger J and U, consistent with the Hubbard model. For both wave functions, a first order metal-insulator transition may be found[12]. Finally, we can plot a phase diagram in J-U plane. The regime $J = 4(t_{mix})^2/U$ with $t_{mix}/U \ll 1$ should describe the physics of the crossover regime in the Hubbard model. We see that if neglecting the high order term, this crossover corresponds to a metal-insulator phase transition.

This paper was organized as follows: In Sec. II, the detailed deduction of the effective model is provided by canonical transformations. In Sec. III, the VMC results for the original Hubbard model and the effective model are presented. In Sec. IV, we give some discussions and conclusions. The mean field theory is arranged in the appendix for giving some feeling to relate our effective model to Laughlin's gossamer superconducting model.

II. HUBBARD MODEL AND ITS LARGE BUT FINITE EFFECTIVE MODEL

A. One-band Hubbard Model

We start from the Hubbard model on a two-dimensional square lattice where the hopping energy may be dependent on the occupation of sites involved[13]. Including the on-site Coulomb interaction, this Hubbard model reads

$$H = T + V = T + U\sum_{i=1}^{L}\nu_i, \tag{1}$$

where L is the number of the site; $\nu_i = n_{i\uparrow}n_{i\downarrow}$, $n_{i\sigma} = c^\dagger_{i\sigma}c_{i\sigma}$ with $c_{i\sigma}$ a spin-σ electron annihilation operator at site i and the kinetic term is given by

$$\begin{aligned}
T &= T_h + T_d + T_{\rm mix}, \qquad (2)\\
T_h &= -\sum_{\langle ij\rangle\sigma} t^h_{ij}(1-n_{i\bar\sigma})c^\dagger_{i\sigma}c_{j\sigma}(1-n_{j\bar\sigma}),\\
T_d &= -\sum_{\langle ij\rangle\sigma} t^d_{ij}n_{i\bar\sigma}c^\dagger_{i\sigma}c_{j\sigma}n_{j\bar\sigma},\\
T_{\rm mix} &= T_+ + T_-\\
&= -\sum_{\langle ij\rangle\sigma} t^{mix}_{ij}n_{i\bar\sigma}c^\dagger_{i\sigma}c_{j\sigma}(1-n_{j\bar\sigma})\\
&\quad -\sum_{\langle ij\rangle\sigma} t^{mix}_{ij}(1-n_{i\bar\sigma})c^\dagger_{i\sigma}c_{j\sigma}n_{j\bar\sigma}.
\end{aligned}$$

Here $T_+(T_-)$ creates (destroys) a double-occupied site. We assume $t^h_{ij} = t^d_{ij} = t$ and $t^{mix}_{ij} = t^m$ for the nearest neighbor sites and vanish otherwise.

B. Effective Model

In large but finite U ($U \gg t_{mix}$), we can treat the T_{mix} term as perturbation, which leads to the t-J model in infinite U limit. An easily pellucid way to arrive at the effective model is via a canonical transformation. In order to define the canonical transformation, we explain our notations. The partial Gutzwiller projection operator

$$\Pi(g) = \prod_i(1-(1-g)\nu_i) = \sum_{D=0}^{N/2} g^D P_D = g^{\hat D}, \tag{3}$$

where $0 \leq g \leq 1$ is the Gutzwiller parameters; N is the electron number[18], $\hat{D} = \sum_i \nu_i$ and

$$P_D = \sum_{\{i_1,...,i_D\}} [\nu_{i_1}...\nu_{i_D} \prod_j{}' (1-\nu_j)]$$

is a projection operator which projects a state into the subspace with a fixed double-occupation number D. $P_0 = \Pi(0)$ is the full Gutzwiller projection operator and $\Pi(1) = 1$. For convenience, we denote

$$P_D(g) = g^D P_D, P_{\eta_i}(g) = \sum_{D \geq i} P_D(g).$$

The first goal of this work is to construct an effective Halmitonian $H_{\rm eff}$ and after the partial Gutzwiller projection, the projected effective Hamiltonian is given by

$$\begin{aligned} \Pi(g) H_{\rm eff} \Pi(g) &= \sum_D P_D(g) H_{\rm eff} P_D(g) \\ &= \sum_D g^{2D} P_D H_{\rm eff} P_D, \end{aligned} \tag{4}$$

i.e., all the off-diagonal part $P_{D'}(g) H_{\rm eff} P_D(g) = 0$ for $D' \neq D$. We shall prove that the result effective Hamiltonian in which all terms keep D-invariance is given by

$$H_{\rm eff} = T_h + T_d + T_p + \mathcal{J} + V, \tag{5}$$

where T_p is a pair hopping kinetic energy and $\mathcal{J}$ is the spin exchange as well as various nearest neighbor interactions, namely,

$$\begin{aligned} T_p &= -\sum_{\langle ij \rangle, \sigma} t_p c^\dagger_{i\sigma} c_{j\sigma} c^\dagger_{i\bar{\sigma}} c_{j\bar{\sigma}}, \\ \mathcal{J} &= \sum_{\langle ij \rangle} J_{ij} (\mathbf{S_i} \cdot \mathbf{S_j} - \frac{1}{4} n_i n_j + \frac{1}{2} n_{i\uparrow} n_{i\downarrow} n_j \\ &+ \frac{1}{2} n_i n_{j\uparrow} n_{j\downarrow} - n_{i\uparrow} n_{i\downarrow} n_{j\uparrow} n_{j\downarrow}). \end{aligned} \tag{6}$$

For $t_{mix}/U \ll 1$, $J_{ij} = J \approx 4t^2_{mix}/U$, $t_p = J$.

The canonical transformation for the Hubbard model to the t-J model has been a standard technique[11]. A detailed review for the canonical transformation can be found in Ref.[19]. Our derivation is a generalization of the $D = 0$ case. Notice that $P_D T_{\rm mix} P_{D'} = \delta_{D',D\pm1} P_D T_{\rm mix} P_{D\pm1}$ and (5) remains D invariant, as well as $\Pi(g)\Pi(g') = \Pi(gg')$, $P_{\eta_D}(g) P_{\eta_D}(g') = P_{\eta_D}(gg')$. Keeping these in mind, we do a partial projection $\Pi(x) H \Pi(x)$ with $x = g^{2/N}$. For large N, x is very close to 1. A straightforward calculation leads to a rewriting of $\Pi(x) H \Pi(x)$

$$\begin{aligned} &\Pi(x) H \Pi(x) = H_0(x) + H^{(1)}_\eta(x), \\ &H_0(x) = H_{diag}(x) + \sum_{D=2} H^{(D)}_\eta(x), \end{aligned} \tag{7}$$

where

$$\begin{aligned} &H_{diag}(x) = \sum_{D=0} P_D(x) H P_D(x), \\ &H^{(D)}_\eta(x) = P_{D-1}(x) T P_D(x) + P_D(x) T P_{D-1}(x). \end{aligned} \tag{8}$$

The purpose of the canonical transformation is to acquire an effective Hamiltonian $H^{(1)}_{\rm eff}$ such that $P_0 H^{(1)}_{\rm eff} P_D = P_D H^{(1)}_{\rm eff} P_0 = 0$ for $D \neq 0$ to the second order of t/U. This $H^{(1)}_{\rm eff}$ is defined by

$$H^{(1)}_{\rm eff} = e^{iS^{(1)}} \Pi(x) H \Pi(x) e^{-iS^{(1)}}. \tag{9}$$

As well-known[11,19], $S^{(1)}$ is determined by the self-consistent condition

$$i H^{(1)}_\eta(x) + [H_0(x), S^{(1)}] = 0$$

and thus the effective Hamiltonian reads

$$\begin{aligned} H^{(1)}_{\rm eff} &= H_0(x) + \frac{i}{2}[S^{(1)}, H^{(1)}_\eta(x)] \\ &- \frac{1}{3}[S^{(1)}, [S^{(1)}, H^{(1)}_\eta(x)]] + ... \end{aligned} \tag{10}$$

Solving the self-consistent condition , $H^{(1)}_{\rm eff}$ in a large U is given by[10,19]

$$P_0 H^{(1)}_{\rm eff} P_0 \approx P_0 H P_0 - \frac{1}{U} P_0 H P_{\eta_1} H P_0, \tag{11}$$

$$\begin{aligned} P_{\eta_1}(x) H^{(1)}_{\rm eff} P_{\eta_1}(x) &\approx P_{\eta_1}(x^2) H P_{\eta_1}(x^2) \\ &+ \frac{1}{U} P_{\eta_1}(x^2) H P_0 H P_{\eta_1}(x^2). \end{aligned} \tag{12}$$

The approximation '$\approx$' in (11) and (12) means the exactness is up to the second order of t/U. Namely, the third term in (10) has been neglected. In fact, the off-diagonal part $P_0 H^{(1)}_{\rm eff} P_{\eta_1}$ vanishes also only up to the second order:

$$\begin{aligned} P_0 H^{(1)}_{\rm eff} P_{\eta_1} &= P_0 H P_{\eta_1} H P_0 H P_{\eta_1} \\ &\approx \frac{1}{U^2} T_- T_+ T_- \sim O(tJ) \end{aligned} \tag{13}$$

is of the third order. The second terms of (11) and (12) may be calculated and given by

$$\begin{aligned} &-\frac{1}{U} P_0 H P_{\eta_1} H P_0 = -\frac{1}{U} P_0 T_- T_+ P_0 \approx P_0 \mathcal{J} P_0, \\ &\frac{1}{U} P_{\eta_1} H P_0 H P_{\eta_1} = \frac{1}{U} P_{\eta_1} T_+ T_- P_{\eta_1} \approx P_{\eta_1} T_p P_{\eta_1} \end{aligned} \tag{14}$$

Thus, up to the second order, we have

$$P_0 H^{(1)}_{\rm eff} P_0 \approx P_0 H_{\rm eff} P_0, \tag{15}$$

$$P_{\eta_1}(x) H^{(1)}_{\rm eff} P_{\eta_1}(x) \approx P_{\eta_1}(x^2)(H + T_p) P_{\eta_1}(x^2). \tag{16}$$

where the approximation '$\approx$', besides up to the second order, also means the three and more sites processes are neglected.

If the non-double occupied constraint is imposed, (16) vanishes because it is related to the double occupation. Eq.(15) gives rise to the common t-J model. However, if the double occupation is allowed, we have to deal with (16). In fact, one can repeats the canonical transformation to (16). We would like to require an effective Hamiltonian $H_{\rm eff}^{(2)}$ whose off-diagonal part $P_1 H_{\rm eff}^{(2)} P_D = P_D H_{\rm eff}^{(2)} P_1 = O(tJ)$ for $D > 1$. For this purpose, one writes

$$\Pi(x) H_{\rm eff}^{(1)} \Pi(x) = P_0 H_{\rm eff}^{(1)} P_0 + \tilde{H}_0(x^2) + H_\eta^{(2)}(x^2), \quad (17)$$

where

$$\tilde{H}_0(x^2) = P_1(x^2)(H+T_p)P_1(x^2) + P_{\eta_2}(x^2)(H+T_p)P_{\eta_2}(x^2).$$

We do a canonical transformation and define

$$H_{\rm eff}^{(2)} = e^{iS^{(2)}} \Pi(x) H_{\rm eff}^{(1)} \Pi(x) e^{-iS^{(2)}}, \quad (18)$$

where $S^{(2)}$ is required to satisfy $P_0 S^{(2)} = S^{(2)} P_0 = 0$ such that $P_0 \Pi(x) H_{\rm eff}^{(1)} \Pi(x) P_0$ is invariant under the transformation and it is self-consistently determined by

$$i H_\eta^{(2)}(x^2) + [\tilde{H}_0(x^2), S^{(2)}] = 0.$$

Hence, similar to (10), one has

$$H_{\rm eff}^{(2)} = P_0 H_{\rm eff}^{(1)} P_0 + \tilde{H}_0(x^2) + \frac{i}{2}[S^{(2)}, H_\eta^{(2)}(x^2)] + ... \quad (19)$$

Projecting $H_{\rm eff}^{(2)} \to \Pi(x) H_{\rm eff}^{(2)} \Pi(x)$ and repeating the similar procedure to deduce (15) and (16), one arrives at

$$\begin{aligned} &P_0 H_{\rm eff}^{(2)} P_0 \approx P_0 H_{\rm eff} P_0, \\ &P_1(x) H_{\rm eff}^{(2)} P_1(x) \approx x^2 P_1 H_{\rm eff} P_1, \\ &P_{\eta_2}(x) H_{\rm eff}^{(2)} P_{\eta_2}(x) \approx P_{\eta_2}(x^3)(H+T_p) P_{\eta_2}(x^3), \end{aligned}$$

for a large U, where the three site processes have been ignored.

Repeating this procedure, we finally have

$$\begin{aligned} \Pi(x) H_{\rm eff}^{(\frac{N}{2})} \Pi(x) &\approx \sum_{D=0} g^{2D} P_D H_{\rm eff} P_D \\ &= \Pi(g) H_{\rm eff} \Pi(g). \end{aligned} \quad (20)$$

The last equality is because $H_{\rm eff}$ is D-invariant. The Gutzwiller parameter is g but not x because we are doing the partial projection in each time canonical transformation. Thus, we end the proof of (4) and (5). Moreover, we see that, in a partial Gutzwiller projection, the variational ground state energy is given by a polynomial of the Guztwiller parameter g in power of $2D$. The coefficient of g^{2D}-term is the ground state energy of the system with a fixed D. Using g as a variational parameter may be convenient for the numerical simulations. In the original Hubbard model, the change of the double occupied number is allowed. We see here that the allowance of this change in a large U is very small. After neglecting the three and more sites processes, the probability of the change of D is in the third order of t/U as eq. (13) shown. Considering the fixed D processes may be helpful to numerical simulations.

III. VARIATIONAL MONTE CARLO RESULTS

A. Variational Wave Functions

The variational wave functions we would like to study are so-called the partially projected RVB state $|\psi_D\rangle = P_D|BCS\rangle$ and the partially projected AF-RVB state $|\psi_D\rangle = P_D|AF\text{-}BCS\rangle$. The BCS state is defined by

$$|BCS\rangle = \prod_k (u_k + v_k c_{k\uparrow}^\dagger c_{-k\downarrow}^\dagger)|0\rangle, \quad (21)$$

where u_k and v_k follows the standard BCS form

$$\begin{aligned} a(k) = \frac{v_k}{u_k} = \frac{\Delta_k}{\xi_k + E_k}, \quad (22) \\ \xi_k = -2(\cos k_x + \cos k_y) - \mu, \quad E_k = \sqrt{\xi_k^2 + \Delta_k^2}, \end{aligned}$$

for the d-wave pairing parameter $\Delta_k = \Delta(\cos k_x - \cos k_y)$. The AF-BCS coexisted state $|AF-BCS\rangle$ is defined by[16]

$$\begin{aligned} |AF-BCS(\Delta_d, \Delta_{af}, \mu)\rangle &= \prod_{k,s} (u_k^{(s)} + v_k^{(s)} d_{k\uparrow}^{(s)\dagger} d_{-k\downarrow}^{(s)\dagger})|0\rangle \\ &\propto \exp\left[\sum_{k,s} \frac{v_k^{(s)}}{u_k^{(s)}} d_{k\uparrow}^{(s)\dagger} d_{-k\downarrow}^{(s)\dagger}\right]|0\rangle, \end{aligned} \quad (23)$$

where

$$\tilde{a}_k^{(\pm)} = \frac{v_k^{(\pm)}}{u_k^{(\pm)}} = \frac{\pm\Delta_d \gamma_k}{(\pm E_k - \mu) + \sqrt{(\pm E_k - \mu)^2 + (\Delta_d \gamma_k)^2}} \quad (24)$$

and $E_k = \sqrt{\epsilon_k^2 + \delta_{af}^2}$, $\epsilon_k = -2(\cos k_x + \cos k_y)$ and $\gamma_k = 2(\cos k_x - \cos k_y)$; and

$$\begin{aligned} d_{k\sigma}^{(+)\dagger} &= \alpha_{k\sigma} c_{Ak\sigma} - \beta_{k\sigma} c_{Bk\sigma}, \\ d_{k\sigma}^{(-)\dagger} &= \beta_{k\sigma} c_{Ak\sigma} + \alpha_{k\sigma} c_{Bk\sigma}, \end{aligned} \quad (25)$$

with

$$\begin{aligned} \alpha_{k\sigma} &= \sqrt{\frac{1}{2}\left(1 - \frac{\sigma\Delta_{af}}{E_k}\right)}, \\ \alpha_{k\sigma} &= \sqrt{\frac{1}{2}\left(1 + \frac{\sigma\Delta_{af}}{E_k}\right)}. \end{aligned} \quad (26)$$

$c_{Ak\sigma}(c_{Bk\sigma})$ is the electron operator on sublattice A(B).

B. Hubbard Model with Asymmetric Hopping

We first make a variational calculation for the original Hubbard model. The energy we want to minimize is given by

$$\begin{aligned} E_H &= Ud + \frac{\sum_D y^D N_D (T_{h,D} + T_{d,D})}{\sum_D y^D N_D} \\ &+ \frac{\sum_D y^{D+1/2} \sqrt{N_D N_{D+1}} T_{D,D+1}^{mix}}{\sum_D y^D N_D}, \end{aligned} \quad (27)$$

where $y = g^2$, $N_D = \langle\psi_D|\psi_D\rangle$ for the partially projected RVB state $|\psi_D\rangle = P_D|BCS\rangle$ or the partially projected AF-RVB state $|\psi_D\rangle = P_D|AF - BCS\rangle$.

The average double occupation number d is given by

$$d = \frac{\sum_{D=0} y^D N_D D/L}{\sum_{D=0} y^D N_D}. \tag{28}$$

And

$$T_{h(d),D} = \frac{\langle\psi_D|T_{h(d)}|\psi_D\rangle}{N_D},$$
$$T^{mix}_{D,D+1} = \frac{\langle\psi_{D+1}|T_+|\psi_D\rangle}{\sqrt{N_D N_{D+1}}} + \frac{\langle\psi_D|T_-|\psi_{D+1}\rangle}{\sqrt{N_D N_{D+1}}}. \tag{29}$$

Let $\{|\alpha_D\rangle\}$ be a set of the basis in the configuration space with a fixed D. The normal factors N_D is given by

$$N_D = \sum_{\alpha_D} \langle\psi_D|\alpha_D\rangle\langle\alpha_D|\psi_D\rangle$$
$$= \sum_{\alpha_D} |\langle\alpha_D|\psi_D\rangle|^2 = \sum_{\alpha_D} |A_{\alpha_D}|^2, \tag{30}$$

where A_{α_D} is just the determinant of the configuration α_D. We are not able to calculate N_D exactly. We use the approximation by taking all probabilities $|A_{\alpha_D}|^2$ to be the same[20,21]. Thus, at half-filling

$$N_D^{RVB} = \frac{L!}{[(N/2-D)!]^2 D!(L-N+D)!}, \tag{31}$$

for the RVB case. In the AF-RVB case, the lattice is divided into two sublattices A and B respectively and

$$N_D^{AF-RVB} = \sum_{N_{A\uparrow}N_{A\downarrow}N_{AD}N_{AE}} \frac{(L/2)!}{N_{A\uparrow}!N_{A\downarrow}!N_{AD}!N_{AE}!}\frac{(L/2)!}{N_{B\uparrow}!N_{B\downarrow}!N_{BD}!N_{BE}!}, \tag{32}$$

where the configurations ($N_{A\uparrow}$,$N_{A\downarrow}$,N_{AD},N_{AE};$N_{B\uparrow}$, $N_{B\downarrow}$,N_{BD},N_{BE}) are corresponding to numbers of spin-up, spin-down, double occupancy and empty sites for each sublattice and subjected to the following constraints:

$$N_{A\uparrow} + N_{A\downarrow} - N_{AD} + N_{AE} = \frac{N}{2}$$
$$N_{B\uparrow} + N_{B\downarrow} - N_{BD} + N_{BE} = \frac{N}{2}$$
$$N_{A\uparrow} + N_{B\uparrow} = N_{A\downarrow} + N_{B\downarrow} = \frac{N}{2}$$
$$N_{AD} + N_{BD} = N_{AE} + N_{BE} = D \tag{33}$$

By using the variational Monte Carlo method[17], we calculate the variational energy (27) by optimizing the variational parameter Δ. The term Ud is not dependent on Δ. For the projected RVB wave function, $T_{h,D}, T_{d,D}$ and $T^{mix}_{D,D+1}$ for several D are depicted in Fig. 1. (The energy unit $t = 1$ is used in all figures through the paper.) The lattice sizes are 10×10 and 12×12, respectively. We use periodic-antiperiodic boundary condition to avoid the degeneracy in Brillouin zone. All data are calculated with more than 10^4 Monte Carlo samples. Although there is a minimum in $T^{mix}_{D,D+1}$ around $\log_{10}\Delta = 0$, the total kinetic energy is minimized after $\log_{10}\Delta < -1.0$ because the minima of $T_{h(d),D}$ are in after $\log_{10}\Delta < -1.0$. Unfortunately, we see that there is very broad minimal flat in variational energy from $\Delta = 0$ to $\log_{10}\Delta \approx -1.0$. Thus, we can not distinguish the metal state is either the Fermi liquid or superconducting state. For the AF-RVB wave function, the trend of $T_{h,D} + T_{d,D}$ and $T_{mix,D,D+1}$ is different. However, in the total energy 27 $T_{h,D} + T_{d,D}$ dominate. So the situation is like the RVB case. The parameters we use are $\log_{10}\Delta = \log_{10}\Delta_d = -0.6$ and the optimal $\log_{10}\Delta_{af} \approx -0.6$[9,22].

Compare the variational energies of the two wave functions, we find that the system is in the projected RVB state for small U and t_{mix} while it is in the projected AF-RVB coexisted state for larger ones. TableI shows the transition when $T_{mix} = 0.6$. The critical line is shown in Fig. 2.

To understand the phase diagram of the system, we shall calculate the optimal average double occupied number d for an appropriate wave function (RVB or AF-RVB) for given t_{mix} and U in the optimal parameters (Δ or Δ_d and Δ_{af}). Substituting (28) into (27) and eliminating y, we get the function E(d). Then, identifying the minimum of E over d, we get the optimal d_0 and E_0. If $d_0 = 0$, the system is in insulating state while if $d_0 > 0$, the system is in metal state. There is a second order phase metal-insulator transition in $t_{mix} = 0$ as show by Fig. 3a. The critical interaction $U_c(0)$ is spotted in Fig. 2. However, when $t_{mix} > 0$,

$$\frac{\partial E(d)}{\partial d}|_{d\to 0} = U + (T_1 - T_0) + \frac{1}{C}\frac{1}{\sqrt{d}}T^{mix}_{0,1} \tag{34}$$

where C is a constant. For any finite t_{mix}, no matter how large U is, it can be found there exists a $d_0 > 0$ so that $\frac{\partial E(d_0)}{\partial d_0} = 0$. As instances, in Fig. 3(b)(c), we plot the d-E curves for $t_{mix} = 0.8$ and $U = 10$ for the RVB state (Fig. 3(b)) and the AF-RVB state (Fig. 3(c)). The dashed curve in Fig. 2 gives the values of (t_{mix}, U) where the $d_0 = 0.01$. For a sufficient small d_0, the system becomes a practical insulator and therefore, there is a metal-insulator crossover as showed by the shade area in Fig. 2. Due to small U, the RVB region is in metal phase. The AF-RVB region is divided into two phases. For a given U, the system is in the insulating phase when t_{mix} is small enough while in metal state when t_{mix} is large.

U	0	1	2	3	4	5	6	4.316
E_{RVB}	-0.835	-0.603	-0.405	-0.242	-0.115	-0.0245	-0.00202	-0.8324
E_{AF-RVB}	-0.795	-0.564	-0.373	-0.221	-0.109	-0.0425	-0.0205	-0.8324

TABLE I: The transition of Hubbard model between RVB and AF-RVB at t_{mix}=0.6. The critical U is 4.316.

C. Effective model

We now begin to examine the effective model. The energy we want to minimize is defined by

$$E = Ud + \frac{\sum_D y^D N_D (T_{h,D} + T_{d,D} + T_{p,D} + J_D)}{\sum_D y^D N_D}, \quad (35)$$

where d defined by (28).

For fixed D, N_D defined by (30), (31) and (32). And $T_{h,D}, T_{d,D}, T_{p,D}, J_D$ is defined by

$$T_{h(d,p),D} = \frac{\langle \psi_D | T_{h(d,p)} | \psi_D \rangle}{N_D},$$
$$J_D = \frac{\langle \psi_D | J | \psi_D \rangle}{N_D} \quad (36)$$

Our strategy is that using the variational Monte Carlo method to minimize E_D for fixed D and fixed electron number N at the half-filling by varying the variational parameter $\log_{10}\Delta$. Then, draw the curves E as the function of d through eqs. (35) and (28), to read out critical U_c and d_c from the shape of the curve for different model parameters U/t and J/t. At the moment, although we still use $J = 4t_{mix}^2/U$, we do not not restrict at $t_{mix}/U \ll 1$. The comparison to the Hubbard model is only valid in the region $t_{mix}/U \ll 1$.

Our variational Monte Carlo carries out on square lattices as in the Hubbard model above, with sites L from 10×10 to 12×12. A periodic-antiperiodic boundary condition is used. All data are calculated with more than 10^4 Monte Carlo samples. In the half-filling, we set the chemical potential $\mu = 0$. The ground state energies E_D are calculated. We show $\vec{S_i} \cdot \vec{S_j}$ for D=0 and D=1 varying as $\log_{10}\Delta$ in Fig.4a for the RVB state. The no-double occupant energy D=0 is the variational ground state energy of the common t-J model. Our result is well consistent with the known results[9,17]. We calculate E_D up to the largest $D = L/2 - 1$, and find that all these energies are almost degeneracy in wide range between $-0.5 \le \log_{10}\Delta \le 0.0$. Using the Monte Carlo estimating energy E_D on 10×10 lattice, we approximate E in (35) by finite sum for $D = 49$ and $\log_{10}\Delta = -0.5$. The error bars for independent Monte Carlo initial configuration are in order of 1% and we do not show them.

The energy of the AF-RVB wave function also can be calculated by variational Monte Carlo method with optimizing both of the model parameters Δ_{af} and Δ_d.We show J_D for D=0 and D=5 in Fig.4b and Fig.4c. The results of D=0 corresponding t-J model at half filling. Our results are consistent with the known results.[16] One can see that for D=0, the energy minimum locates in a deep valley.

We also analyze the two wave functions' finite-size scaling of D=0 which corresponds to Heisenberg model. The results are show in Fig.5. All the data but the 16×16 of AF-RVB, which is only one datum since it is required very long time to get one result, are average of 5 independent calculations. One can see that for Heisenberg model the energies of AF-RVB are deeper than those of RVB.

For a pair of fixed J and U, we can compare the variational energies corresponding to both wave functions(Tab.II). In this way, the J-U plane can be divided into two regions: RVB and AF-RVB, which is similar to the case in the last subsection for the Hubbard model.

For a given type wave function, we look for the possible metal-insulator transition. First, like the case in Hubbard model, there is a second order phase transition when $J = 0$. If $J > 0$, due to the vanishing of T^{mix} term, there are first order phase transitions in a given type wave function. Fig. 6 gives an example of the first order metal-insulator transition. In Fig. 8, we show the relation between the critical U_c or J_c and the critical double occupied concentration d_c for the RVB wave function. In this way, we can determine the critical $J_c - U_c$ line in J-U plane. Figs. 7(a)(b) show the critical $J_c - U_c$ lines for the RVB and AF-RVB wave functions. They are quite similar. Combining these two phase diagrams together with the region-dividing picture mentioned above, we depict the comprehensive phase diagram (Fig. 9(a)). In the RVB region, due to small J and U, the system is in metal state. In the AF-RVB region, the system is basically in an insulating phase. For $J \ge 0.5$, there is a phase which may be a AF-RVB metal state. Since the optimal variational parameters Δ and Δ_d are not zero, the metal state may be a superconducting state. Converting $J \to t_{mix}$ (see Fig. 9(b)), we find that for small t_{mix}, the phase diagram is consistent with the crossover picture in the Hubbard model .

IV. DISCUSSIONS AND CONCLUSIONS

We have investigated the Hubbard model with the hopping asymmetry and deduced an effective theory for large but finite U. Based on two types of the variational wave functions, the phase diagram of both models are depicted by the variational Monte Carlo method. For the Hubbard model, we found it is difficult to determine the exact critical boundary of the phase transition of metal-insulator. Moreover, the superconducting behavior in

U	1	2	3	4	5	6	3.512
E_{RVB}	-0.656	-0.491	-0.381	-0.34	-0.34	-0.34	-0.3494
E_{AF-RVB}	-0.616	-0.457	-0.365	-0.34943	-0.34943	-0.34943	-0.3494

TABLE II: The transition of t-J-U model between RVB and AF-RVB at J=0.3. The critical U is 3.512. The critical U of RVB M-I transition is 3.8, and that of AF-RVB is 3.45.

the metal phase was not clear. The effective model is a finite but large U extension of the t-J model. This model captures both the charge and exchange correlation. The phase diagram of this model clearly shows a metal-insulator phase transition. Due to non-zero optimal Δ and Δ_d, the metal state may be superconducting, which leads to the possibility of the gossamer superconductivity in the framework of the hopping asymmetry Hubbard model.

The relation to the gossamer superconductivity can also be seen from the mean field state of our theory. The basic idea to go this mean field state has been explained in our previous preprint[23]. Here we present a renewed version of the mean field state. We only try to show our mean field theory may formally be equivalent to Laughlin's gossamer superconducting model. We do not intent to go more analysis such as the stability of our mean field state against other possible instabilities before we work out some more sophisticated issues. We put this formal identification into Appendix A.

ACKNOWLEDGEMENTS

The authors are grateful for the useful discussions to Jingyu Gan, Jinbin Li, Zhaobin Su, Tao Xiang, Lu Yu and F. C. Zhang. One of the authors (Y.W.) would like to thank Lei Zhang at C.I.T. for some mathematical help. This work was supported in part by the NSF of China. Part of the computation of this work was performed on the HP-SC45 Sigma-X parallel computer of ITP and ICTS,CAS.

APPENDIX A: MEAN FIELD STATE

We outline the mean field state of our model in this appendix. Due to the paring hopping is of the order J, we neglected it in our mean field theory. Introducing two correlation functions $\Delta_{ij} = \langle c_{i\downarrow}c_{j\uparrow} - c_{i\uparrow}c_{j\downarrow}\rangle_0, \chi_{ij} = \langle c^\dagger_{i\uparrow}c_{j\uparrow} + c^\dagger_{i\downarrow}c_{j\downarrow}\rangle_0$, the $U(1)$ symmetry of $H_{\rm eff}$ is broken by a decomposition of the four particle terms[23]. According to Δ_{ij} and χ_{ij}, the mean field Hamiltonian of (5) is given by

$$\begin{aligned} H_{\rm MF} &= -\sum_{\langle ij\rangle\sigma}(t^h_{ij} + t^{(1)}_{ij}(n_{i\bar\sigma}+n_{j\bar\sigma}) + t^{(2)}_{ij}n_{i\bar\sigma}n_{j\bar\sigma})c^\dagger_{i\sigma}c_{j\sigma} \\ &+ \sum_{\langle ij\rangle\sigma}(J_{ij} + J^{(1)}_{ij}(n_{i\sigma}+n_{j\bar\sigma}) + J^{(2)}_{ij}n_{i\sigma}n_{j\bar\sigma}) \\ &\times (-1)^\sigma(\Delta^\dagger_{ij}c_{i\sigma}c_{j\bar\sigma} + \Delta_{ij}c^\dagger_{j\bar\sigma}c^\dagger_{i\sigma}) \\ &+ U\sum_i n_{i\uparrow}n_{i\downarrow} - \sum_{\langle ij\rangle}2J_{ij}(1-A)n_{i\uparrow}n_{i\downarrow} \qquad \text{(A1)} \\ &- \sum_{\langle ij\rangle}J_{ij}(A|\Delta_{ij}|^2 + \frac{1}{2}(1-B)|\chi_{ij}|^2)(n_i+n_j) \\ &+ \sum_{\langle ij\rangle\sigma}J_{ij}(\frac{A}{2}|\Delta_{ij}|^2 n_{i\sigma}n_{j\bar\sigma} + \frac{1-B}{2}|\chi_{ij}|^2 n_{i\sigma}n_{j\sigma}), \end{aligned}$$

where the parameters are given by

$$\begin{aligned} &J^{(1)}_{ij} = \frac{A}{2}J_{ij}, \quad J^{(2)}_{ij} = -\frac{B}{2}J_{ij}, \\ &t^{(1)}_{ij} = -t^h_{ij} - (1-A)\chi_{ji}J_{ij}, \qquad \text{(A2)} \\ &t^{(2)}_{ij} = t^h_{ij} + t^d_{ij} - (1-B)\chi_{ji}J_{ij}. \end{aligned}$$

A and B are the variantional parameters to be determined. On the other hand, we write down Laughlin's gossamer superconducting Hamiltonian

$$H_G - \mu_R N = \sum_{\mathbf{k}} E_{\mathbf{k}}\tilde b^\dagger_{\mathbf{k}\sigma}\tilde b_{\mathbf{k}\sigma}, \qquad \text{(A3)}$$

where μ_R is renormalized chemical potential, $E_k = \sqrt{(\epsilon_k - \mu_R)^2 + \Delta_k^2}$ and $\tilde b_{\mathbf{k}\sigma} = \Pi(g)b_{\mathbf{k}\sigma}\Pi^{-1}(g)$ for $b_{\mathbf{k}\uparrow} = u_{\mathbf{k}}c_{\mathbf{k}\uparrow} + v_{\mathbf{k}}c^\dagger_{-\mathbf{k}\downarrow}$ and $b_{\mathbf{k}\downarrow} = u_{\mathbf{k}}c_{\mathbf{k}\downarrow} - v_{\mathbf{k}}c^\dagger_{-\mathbf{k}\uparrow}$ annihilate the BCS state. Expressing explicitly (A3) by the electron operators[6,23], we have

$$\begin{aligned} H_G - \mu_R N = &-\sum_{\langle ij\rangle\sigma}[t^G_{ij} + t^{G(1)}_{ij}(n_{i\bar\sigma}+n_{j\bar\sigma}) \\ &+ t^{G(2)}_{ij}n_{i\bar\sigma}n_{j\bar\sigma}] + \sum_{\langle ij\rangle\sigma}J_{ij}[1 + \frac{1}{2}\alpha\beta(n_{i\bar\sigma}+n_{j\bar\sigma}) \\ &- \alpha\beta n_{i\bar\sigma}n_{j\bar\sigma}](-1)^\sigma(\Delta^\dagger_{ij}c_{i\sigma}c_{j\bar\sigma} + \Delta_{ij}c^\dagger_{j\bar\sigma}c^\dagger_{i\sigma}) \\ &+ U_G\sum_i n_{i\uparrow}n_{i\downarrow} - \mu_G N \qquad \text{(A4)} \end{aligned}$$

where $\alpha = 1-g$ and $\beta = (1-g)/g$ and

$$\begin{aligned} t_{ij}^{G} &= t_{ij}^{h}, \\ t_{ij}^{G(1)} &= -\sum_{k} \frac{E_{\mathbf{k}}}{M}(\alpha v_{\mathbf{k}}^2 + \beta u_{\mathbf{k}}^2) e^{i\mathbf{k}\cdot(\mathbf{r}_i-\mathbf{r}_j)} \\ t_{ij}^{G(2)} &= \sum_{k} \frac{E_{\mathbf{k}}}{M}(\alpha^2 v_{\mathbf{k}}^2 - \beta^2 u_{\mathbf{k}}^2) e^{i\mathbf{k}\cdot(\mathbf{r}_i-\mathbf{r}_j)}, \\ J_{ij}\Delta_{ij} &= \sum_{\mathbf{k}} \frac{E_{\mathbf{k}}}{M} u_{\mathbf{k}} v_{\mathbf{k}} e^{i\mathbf{k}\cdot(\mathbf{r}_i-\mathbf{r}_j)}, \end{aligned} \tag{A5}$$

and $U_G = \frac{1}{M}\sum_{\mathbf{k}} E_k[(2\beta+\beta^2)u_k^2 + (2\alpha-\alpha^2)v_k^2], \mu_G = \frac{1}{M}\sum_{\mathbf{k}} E_k[(2\alpha+1)v_k^2 - u_k^2]$. If we identify the t-J-U model to the gossamer superconducting model in the mean field level, one requires

$$\begin{aligned} &A = \alpha\beta, \quad B = 2\alpha\beta, \\ &t^{G(1)} = -t_{ij}^{h} - (1-\alpha\beta)\chi_{ji}J_{ij}, \\ &t_{ij}^{G(2)} = t_{ij}^{h} + t_{ij}^{d} - (1-2\alpha\beta)\chi_{ji}J_{ij}, \end{aligned} \tag{A6}$$

and $\mu_R + \mu_G = J(12A|\Delta_\tau|^2 + 8(1-B)|\chi_\tau|^2) + \mu, U = U_G + 8J(1-A)$.

Although we have made a formal equivalence between our mean field state Hamiltonian to Laughlin gossamer superconducting Hamiltonian, we note that the hopping parameters $t^{G(1,2)}$ have run out of the practical range in the real materials. Thus, to show the system described by the t-J-U model has a gossamer superconducting phase described by Laughlin gossamer superconducting Hamitonian, a renormalization group analysis is required. We do not touch this aspect in this work. However, we can believe there is such a superconducting phase in our theory if $U < U_c$ because the superconducting paring parameter is determined by the optimal exchange energy as in the common t-J model. The renormalization of the hopping parameters is believed to affect the normal dissipation process only.

[1] J. Hubbard, Proc. R. Soc. London Ser. A **276** 238 (1963).
[2] P. W. Anderson, Science **235**, 1196(1987). F. C. Zhang and T. M. Rice, Phys. Rev. B **37**, 3759 (1988).
[3] R. B. Laughlin, E-preprint: cond-mat/0209269.
[4] T. C. Hua, Phys. Rev. B **41**, 11379 (1990).
[5] F. C. Zhang, Phys. Rev. Lett. **90**, 207002 (2003).
[6] B. A. Bernevig, R. B. Laughlin, D. I. Santiago, Phys. Rev. Lett. **91**, 147003 (2003).
[7] S. Daul, D. J. Scalapino, and S. R. White, Phys. Rev. Lett. **84**, 4188 (2000). L. Arrachea and A. A. Aligia, Phys. Rev. B **61**, 9686. E. Plekhanov, S. Sorella, and M. Fabrizio, Phys. Rev. Lett. **90**, 187004 (2003).
[8] W. F. Brinkman and T. M. Rice Phys. Rev. B **2**, 4302 (1970).
[9] C. Gros, Phys. Rev B **38**, 931 (1988); T. K. Lee and S. Feng, Phys. Rev. B **38**,(1988).
[10] J. Hirsch, Phys. Rev. Lett. **54**, 1317 (1985).
[11] See, e.g., K. A. Chao, J. Spalek, and A. M. Oles, J. Phys. C **10**, L271 (1977).
[12] J. Y. Gan, F. C. Zhang, and Z. B. Su, E-preprint: cond-mat/0308398.
[13] See, e.g., L. Arrachea, A. A. Aligia, and E. R. Gagliano, Phys. Rev. Lett. **76**, 4396 (1996) and references therein.
[14] T.Giamarchi and C.Lhuillier, Phys. Rev. B **43**,12943 (1991).
[15] J. Y. Gan, F. C. Zhang, and Z. B. Su, Phys. Rev. B **71**, 014508 (2005)
[16] A. Himeda and M. Ogata, Phys. Rev. B **60**, 9935 (1999).
[17] A review for the VMC to the t-J model, see, C. Gros, Ann. Phys. (N. Y.) **189**, 53 (1989).
[18] The summation over D runs from 1 to L in general. However, for a fixed particle number N, the highest number of the double occupied sites is $N/2$.
[19] A. P. Balachandran, E. Ercolessi, G. Morandi and A. M Srivastava, Intl. J. Mod. Phys. B **4**, 2057(1990).
[20] D. Vollhardt, Rev. Mod. Phys. **56**, 99 (1984).
[21] T. Ogawa, K. Kanda, and T. Matsubara, Prog.Theor.Phys. **53**, 614 (1975).
[22] M. Ogata and A. Himeda, E-preprint: cond-mat/0003465.
[23] Yue Yu, E-preprint: cond-mat/0211131.

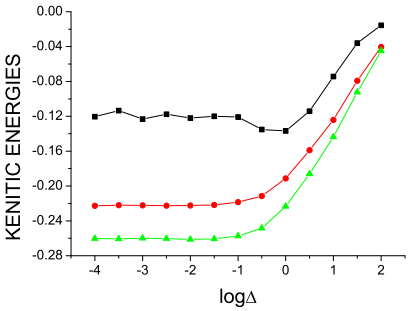

(a)

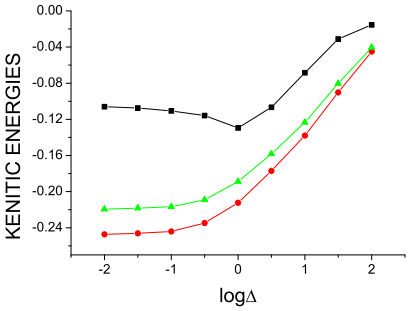

(b)

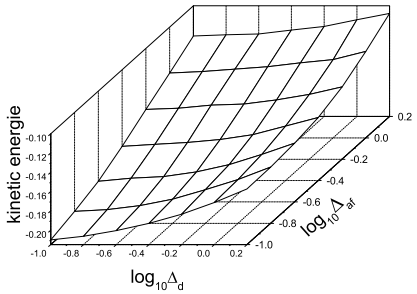

(c)

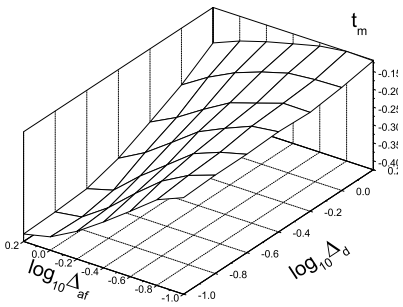

(d)

FIG. 1: (a)(b)The kinetic energies $T_{h,D} + T_{d,D}$ and $T_{mix,D,D+1}$ of RVB as functions of $\log_{10}\Delta$. (a) $T_{-,5,6} + T_{+,6,5}$ (squares), $T_{h,5} + T_{d,5}$ (circles) and $T_{h,6} + T_{d,6}$ (triangles) in a 10×10 lattice. (b) $T_{-,7,8} + T_{+,8,7}$ (triangles), $T_{h,7} + T_{d,7}$ (squares) and $T_{h,8} + T_{d,8}$ (circles) in a 12×12 lattice.(c)(d)The kinetic energies $T_{h,D} + T_{d,D}$ and $T_{mix,D,D+1}$ of AF-RVB as functions of $\log_{10}\Delta_d$ and $\log_{10}\Delta_{af}$ in a 10×10 lattice.(c)$T_{h,5} + T_{d,5}$.(d) $T_{-,5,6} + T_{+,6,5}$. Note that for the different trend between $T_{h,D} + T_{d,D}$ and $T_{mix,D,D+1}$, we change the view of $T_{mix,D,D+1}$.

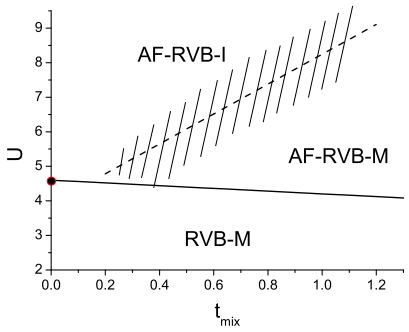

FIG. 2: The possible phase diagram of the Hubbard model. The solid line divides the t_{mix}-U plane into the RVB and AF-RVB regions. The RVB region is in metal state (RVB-M). There is a crossover from metal to insulator in AF-RVB region(AF-RVB-M to AF-RVB-I). The spot on the U-axis ($t_{mix} = 0$) is the metal-insulator phase transition point $U_c(0)$. The shade area is the crossover region and along the dashed curve, $d_0 = 0.01$.

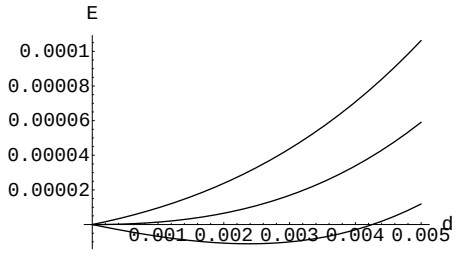

(a)

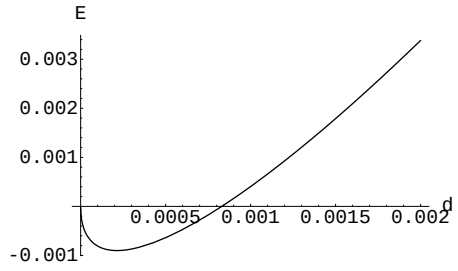

(b)

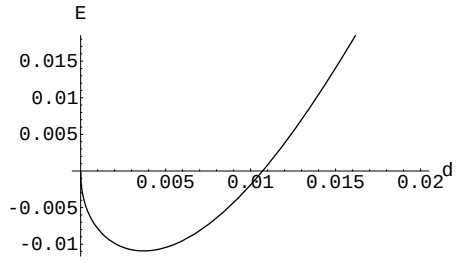

(c)

FIG. 3: The d-E curves of Hubbard model. (a) $t_{mix} = 0$. The different curves are corresponding to different U. Lower curve has a smaller U. The second phase transition happens at $U_c(0) = 4.5678$. (b) and (c) are d-E curves for RVB state and AF-RVB state at $t_{mix} = 0.8$ and $U = 10$, respectively.

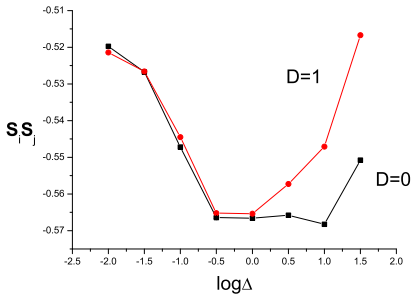

(a)

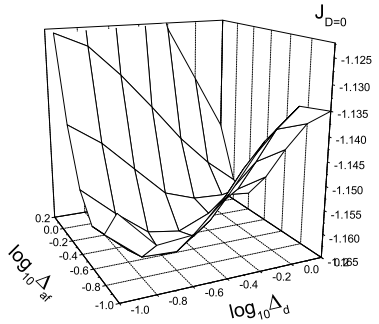

(b)

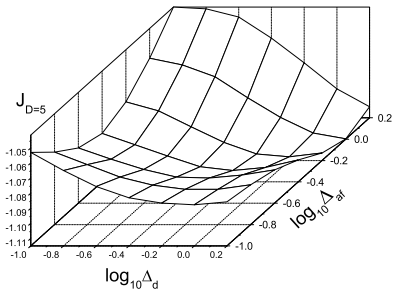

(c)

FIG. 4: The variational energy for fixed D varying as the variational parameter $\log_{10}\Delta$ for RVB(a), $\log_{10}\Delta_{\rm d}$ and $\log_{10}\Delta_{\rm af}$ for AF-RVB(b)(c).

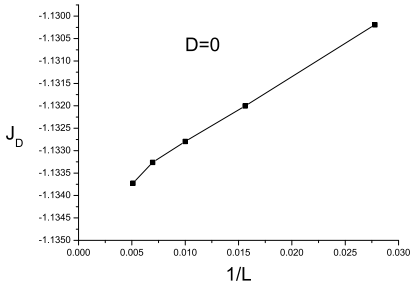

(a)

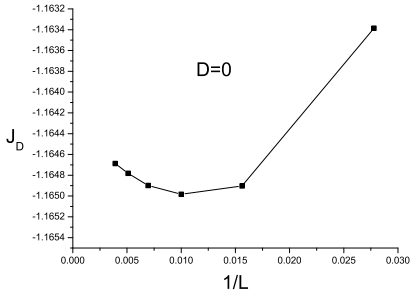

(b)

FIG. 5: Finite-size scaling of RVB at $\log_{10}\Delta$=-0.5(a) and AF-RVB at $\log_{10}\Delta_d$=-0.6 and $\log_{10}\Delta_{af}$=-0.6(b).Where L is the lattices size.

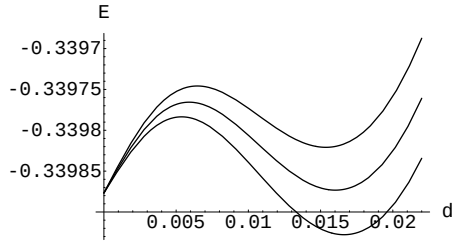

FIG. 6: The total energy E averaged in RVB variational wave function varying with the double occupant concentrate d for $J = 0.3$ and U=3.804, 3.8007, 3.7974 from the upmost to the lowest, respectively. The critical $U_c = 3.8007$ and $d_c = 0.0135$ in this case.

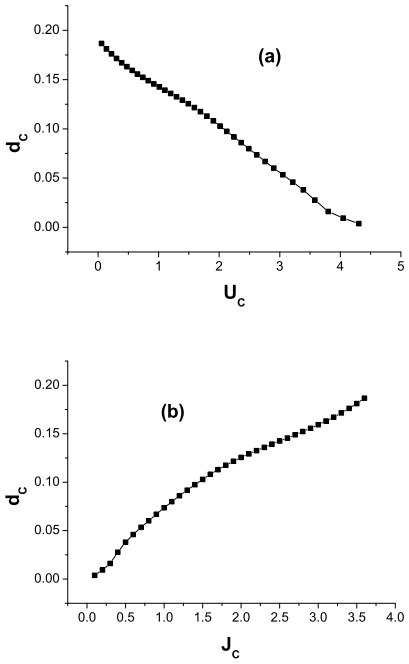

FIG. 7: The critical concentration d_c for the RVB state (a) U_c-d_c curve; (b) J_c-d_c curve.

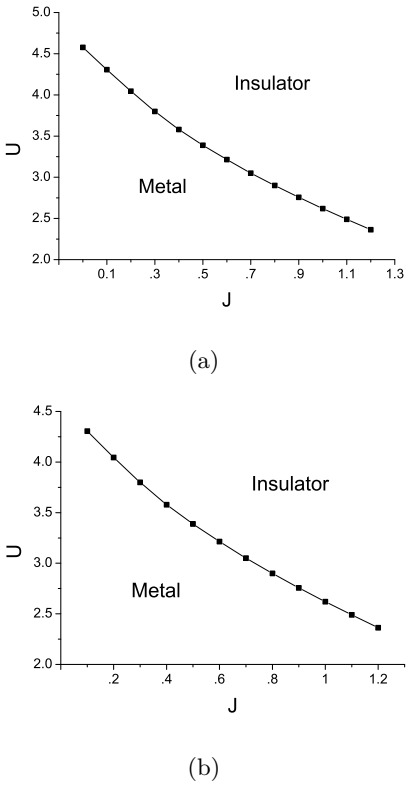

FIG. 8: Phase diagrams for different variational wave functions. (a) for the RVB wave function; (b) for the AF-RVB wave function

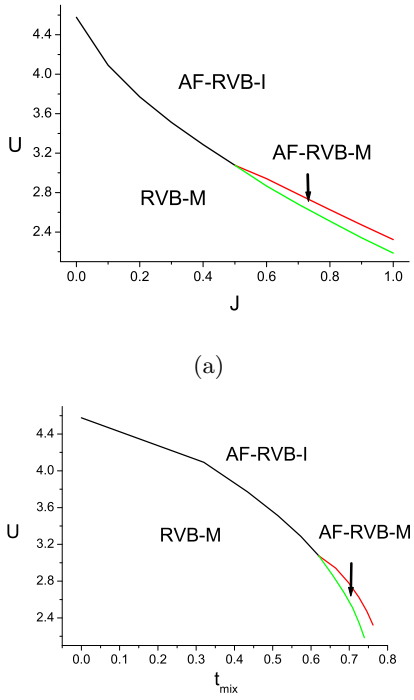

FIG. 9: Phase diagrams of the effective model (a) the phase diagrams of the system in the J-U plane.(b) converting (a) to t_{mix}-U.